

Anomalous lithium storage in a novel nanonet composed by SnO₂ nanoparticles and poly(ethylene glycol) chains†

Huanming Xiong,^a Weizhi Shen,^a Binkun Guo,^b Shouhang Bo,^a Wangjun Cui,^a Liquan Chen,^b Hong Li^{*b} and Yongyao Xia^{*a}

Received 20th October 2010, Accepted 4th January 2011

DOI: 10.1039/c0jm03558k

A series of PEG–SnO₂ nanocomposites has been investigated as anode materials for lithium batteries. They exhibited an unexpectedly high lithium storage over the theoretical capacity of SnO₂. The origin of such extra capacity cannot be interpreted by the conventional lithium storage mechanisms of anode materials.

Polymers can be used as electrode materials in lithium batteries through two storage mechanisms. One is anion insertion into polymers such as polyacetylene, polyaniline and polypyrrole–polythiophene.^{1–4} The electrochemical potentials of these materials range from 3.0 to 4.8 V vs. Li⁺/Li, exhibiting the capacities of 70–90 mA h g^{−1}. Another mechanism is based on direct bonding between lithium and polymers, such as Li–O bonds in poly(dimercaptothiadiazole)^{1,4} and Li–S bonds in poly(2,5-dihydroxy-1,4-benzo-quinone-3,6-methylene),⁵ which show potentials of 2.8 and 3 V and capacities of 375 and 340 mAh g^{−1}, respectively. Recent reports indicate that some organic compounds composed of lithium and small ligands, such as lithium oxocarbon, lithium terephthalate and lithium *trans*–*trans*-muconate can store lithium reversibly through direct bonding of lithium with oxygen on the chain.^{4,6} The common feature of these polymer electrode materials is that they all have conjugated double bonds.

Poly(ethylene glycol) (PEG) and polyethylene oxide (PEO) with the common –CH₂CH₂O– units, have been widely investigated as electrolytes in lithium batteries.^{7–9} The ionic transport mechanism is Li⁺ ions move from one coordination site to another revolved by the polymer chains.^{8,9} On one hand, the reaction between lithium and PEG is not reversible at ambient conditions. On the other, PEO has been proven to be stable even in contact with lithium at 60 °C.¹⁰ Hence, there are no literature reports that ethylene oxide units in polymers can be used for

reversible lithium storage so far. Here, we show that a novel nanonet composed of SnO₂ nanoparticles and PEG chains exhibits much higher lithium storage than the typical SnO₂ nanoparticles. It seems that good electronic contact between PEG and SnO₂ nanoparticles can activate inert ethylene oxide units for reversible lithium storage.

Experimentally, the fresh SnO₂ obtained by hydrolyzing a 0.5 M SnCl₄ aqueous solution in a poly(tetrafluoroethylene) (PTFE)-lined autoclave at 160 °C for 2 h, were centrifuged and subsequently dispersed in liquid PEG under continuous stirring. The formed sols were then precipitated and washed with ethanol under sonication. Afterwards, the white precipitate was redispersed in PEG (*M_w* = 200, 400, 600, 800 and 1000 g mol^{−1}) or PEGME (polyethylene glycol methyl ether, *M_w* = 350 g mol^{−1}), and followed by heating in autoclaves at 180 °C for 1 h. The final product was obtained by adding excess ethanol and the precipitates were washed with ethanol. Finally, the white products were dried under high vacuum at 80 °C for 24 h to remove water and ethanol. The PEG–SnO₂ samples were analyzed by the thermogravimetric technique on a Perkin-Elmer TGA 7 thermal analyzer in air with a heating rate of 10 °C min^{−1}. Additionally, the diluted acetonitrile solutions of different samples were dropped on copper meshes and dried for taking high-resolution images on a JEOL JEM-2010 transmission electron microscope operating at 200 kV.

For lithium cell tests, the electrodes contained 70 wt% active material (PEG–SnO₂, PEGME–SnO₂, PEG and SnO₂), 20 wt% acetylene black and 10 wt% PVDF. Cu foil was used as the current collector. The electrochemical tests were taken on a coin-type cell (CR2016) in an argon filled glove box. A lithium pellet was used as the counter electrode. The electrolyte solution was 1 M LiPF₆ dissolved in ethylene carbonate (EC)/dimethyl carbonate (DMC)/ethylene methyl carbonate (EMC) (1 : 1 : 1 in volume). The typical mass loading of the active material was approximately 10 mg cm^{−2}. The cells were cycled at a constant current density of 0.3 mA cm^{−2} between 0.0 and 2.0 V. The capacity of each active material was calculated according to the electrode performance.

The TEM images in Fig. 1 show that the SnO₂ particles are well crystallized with diameters of 4–5 nm and these nanocrystals aggregate closely due to the PEG linkage. The weight ratio of SnO₂ in the PEG400–SnO₂ composite was 29.4 wt% according to the thermogravimetric (TG) measurement. The

^aDepartment of Chemistry and Shanghai Key Laboratory of Molecular Catalysis and Innovative Materials, Institute of New Energy, Fudan University, Shanghai, 200433, P.R. China. E-mail: yxia@fudan.edu.cn; Fax: (+86)-21-55664177

^bBeijing National Laboratory for Condensed Matter Physics, Institute of Physics, Chinese Academy of Sciences, Beijing, 100190, China. E-mail: hli@aphy.iphy.ac.cn; Fax: (+86)-21-55664177

† Electronic supplementary information (ESI) available: electrochemical charge/discharge curves of lithium cells for the control experiments and cyclic voltammograms of the PEG400–SnO₂ composites. See DOI: 10.1039/c0jm03558k

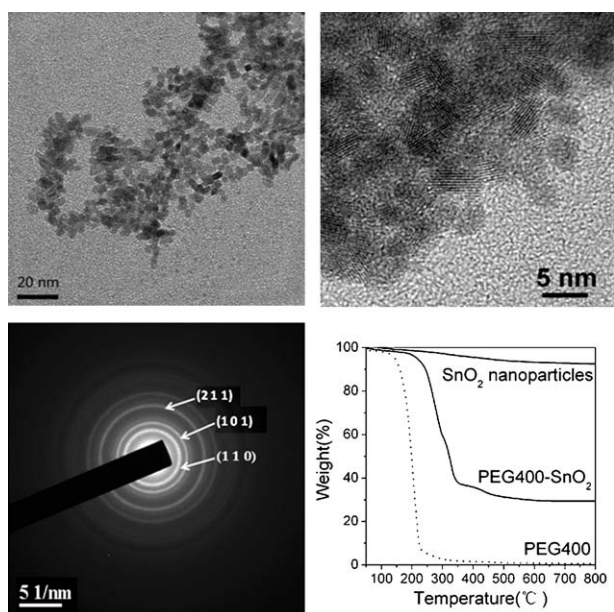


Fig. 1 The upper HRTEM images of the PEG400-SnO₂ nanoparticles show that these nanocrystals are crosslinked by PEG. The lower ED patterns (left) suggested that the as-prepared materials are polycrystalline with a cassiterite structure. The TG curves show the decomposition of PEG400-SnO₂ and PEG400 during heating scans.

weight ratio of SnO₂ in the composites depends on the molecular weight of the grafted PEG, as shown in Table 1. The TG measurements also show that the decomposition temperatures of the PEG-SnO₂ composites are higher than the corresponding PEG, indicative of strong interactions between the nanocrystals and PEG molecules.

As demonstrated in our previous work, many metal oxide nanoparticles prepared by hydrothermal methods, such as TiO₂ and SnO₂, can form polyether-grafted composites through chemical covalent bonds after the exchange reactions on the particle surfaces.¹¹⁻¹³ The IR spectra of SnO₂, PEG and PEG-SnO₂ nanocomposites are shown in Fig. 2. Three changes in the spectra prove that PEG molecules have been modified onto SnO₂ nanoparticles. First, the typical absorption at 1110 cm⁻¹ (CH₂-O-CH₂ stretching) and many IR absorption bands representing C-H vibrations (2875, 1460, 1350, 1295, 1250 and 950 cm⁻¹) are obvious in the PEG-SnO₂ curve. Secondly, the Sn-O-Sn symmetric stretching at 667 cm⁻¹ the inside of the SnO₂ nanoparticles remains unchanged after exchange reactions while the Sn-O asymmetric stretching at 543 cm⁻¹ on the SnO₂ surface decreases to 528 cm⁻¹, indicating that a new covalent bond has formed on the SnO₂ surface.¹³⁻¹⁵ In the meantime, the Sn-O asymmetric stretching band becomes

Table 1 The Li-storage capacity of different PEG-SnO₂ composites

M _w of PEG	SnO ₂ in PEG-SnO ₂ (wt%)	Expected capacity for Li _{4.4} Sn (mA h g ⁻¹)	Our data at the 2nd cycle (mA h g ⁻¹)	Extra capacity (mA h g ⁻¹)
200	52.1	410	768	358
400	29.4	231	639	408
600	21.6	169	442	273
800	15.5	122	300	178
1000	15.1	119	226	107

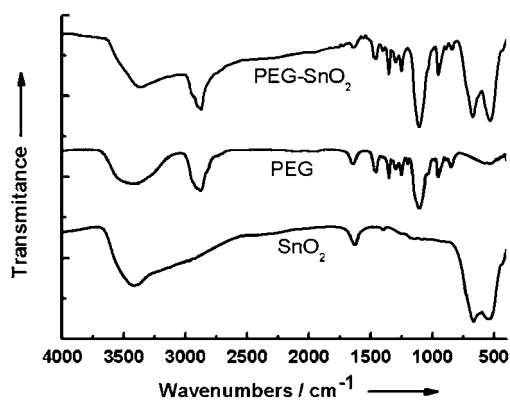


Fig. 2 IR Spectra of SnO₂, PEG and PEG-SnO₂ composites.

sharp in PEG-SnO₂ curve, indicating that the random OH groups chemically adsorbed on the nanoparticle surfaces have been replaced by uniform PEG molecules. Thirdly, the OH absorption of PEG at about 3500 cm⁻¹ has changed significantly when PEG molecules are modified on the SnO₂ surface because part of the OH groups have been exhausted after the exchange reactions. These changes of IR vibrations confirm that PEG molecules have been modified on nanoparticle surfaces through covalent bonds,¹⁶ in accordance with the thermal analyses. Since one PEG molecule has two OH end groups, *i.e.*, one polymer chain is able to connect two SnO₂ nanoparticles, and thus, a novel nanonet composed of numerous nanoparticles and polymer chains will form finally. In contrast, the TEM images of PEGME-SnO₂ showed the nanoparticles were monodispersed.¹¹

The voltage profiles of the PEG400, SnO₂ and the PEG-SnO₂ nanocomposite electrodes in lithium half cells are shown in Fig. 3a-c respectively. PEG400 shows an initial lithium storage capacity of 300 mA h g⁻¹, a reversible capacity of 75 mA h g⁻¹ and an initial coulombic efficiency of 25% (Fig. 3a). The typical initial and reversible capacity of carbon black is about 400 mA h g⁻¹, and 150 mA h g⁻¹ respectively. Therefore, the contribution from the carbon black to the initial capacity and reversible capacity are 80 mA h g⁻¹ and 30 mA h g⁻¹ respectively, because

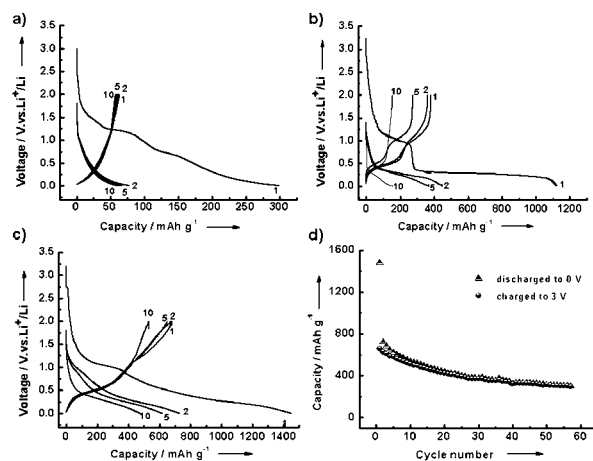


Fig. 3 Electrochemical charge-discharge cycling performance of (a) PEG400, (b) SnO₂ nanoparticles and (c) PEG400-SnO₂ nanocomposites. (d) A capacity attenuation curve of the PEG400-SnO₂ nanocomposites.

the ratio of the carbon black in the electrode composition is 20 wt%. The initial capacity of 300 mA h g⁻¹ could be partially related to the formation of the solid electrolyte interphase (SEI) film on the surface of the PEG/carbon black composite. The initial capacity of SnO₂ (Fig. 3b) obtained by the hydrothermal reaction is 1105 mA h g⁻¹, slightly less than 1480 mA h g⁻¹ of the theoretical lithium storage capacity for the formation of Li_{4.4}Sn and Li₂O. The reversible capacity of our SnO₂ nanoparticles is 480 mA h g⁻¹, less than 778 mA h g⁻¹ of the theoretical capacity for forming Li_{4.4}Sn reversibly. However, the PEG400–SnO₂ nanocomposite (Fig. 3c) shows an initial lithium storage capacity of 1450 mA h g⁻¹, a reversible capacity of 700 mA h g⁻¹ and an initial coulombic efficiency of 47%. This reversible capacity is much larger than the expected value of 231 mA h g⁻¹ for forming Li_{4.4}Sn, as shown in Table 1. Our control experiments show the PEG–SnO₂ nanocomposites with different molecular weight of PEGs have similar charge/discharge profiles except for capacities (see Fig. S1†). If the reversible capacity only results from the formation of an Li_{4.4}Sn alloy, there must be an extra capacity in each PEG–SnO₂ sample. In fact, the real extra capacities are even larger than the values calculated in Table 1 because the theoretical capacity of Li_{4.4}Sn is actually not achieved, as shown in Fig. 3b. Our control experiments confirmed the extra lithium storage in the nanonets is neither from carbon nor from PEG, and it does not appear in the physical mixtures of PEG and SnO₂ (see Fig. S2†). Moreover, it cannot be ascribed to the high dispersion of SnO₂ nanoparticles because the SnO₂ counterparts protected by PEGME do not show any extra capacities.

In order to explore the origin of such high extra capacities in the PEG–SnO₂ nanonets, PEG molecules of different molecular weights were modified on SnO₂ nanoparticles. In Table 1, the higher PEG molecular weight renders the lower SnO₂ content in the PEG–SnO₂ composites. If the SnO₂ in the PEG–SnO₂ is all transformed into the Li_{4.4}Sn alloy and there is no other lithium storage, the expected capacities of the PEG–SnO₂ will be the reversible capacities of the Li_{4.4}Sn, which are listed in the third column of Table 1. Obviously, the actual capacity of each sample is much higher than the Li_{4.4}Sn contribution. Although lithium is able to react with the OH groups of PEG and those on the SnO₂ surface, such a reaction will release hydrogen gas irreversibly in the first cycle. Moreover, the extra capacity calculated according to the second cycle of the battery performance, reaches a maximum when the PEG molecular weight is 400, indicating that the origin of the extra storage is neither simply related to the PEG molecular weight nor determined by the PEG weight ratio.

The interfacial storage mechanism, proposed by Maier and co-workers,¹⁷ suggested that extra lithium could be stored at the interfacial regions between two phases when lithium cannot be further accommodated by two host phases. In those cases, typical voltage profiles show a sloped feature.^{18–21} However, in Fig. 3c, lithium is stored in two obvious plateau regions below 1.0 V and above 1.0 V. The capacity for the first plateau region below 1.0 V is about 400 mA h g⁻¹, corresponding to reversible delithiation reaction of Li–Sn alloy. The second voltage plateau at 1.0–2.0 V contributes about 300 mA h g⁻¹ capacity, which cannot be ascribed to the interfacial lithium storage. Another possibility for unexpected lithium storage behavior is related

to the reversible formation/decomposition of the SEI film. According to our previous research, the reversible formation and decomposition of the SEI film is harmful for achieving better cyclic performance.²² However, the capacity retention is quite good, as shown in Fig. 3d. Therefore, the extra capacity of our PEG–SnO₂ cannot be ascribed to the SEI film either.

After excluding those possibilities based on the popular mechanisms, we speculate that lithium is stored in the PEG–SnO₂ nanocomposites, where the crosslinked SnO₂ particles pave the electron paths and the revolved EO segments provide the coordination centers. When the composite electrode is charged, those Li⁺ ions coordinated with EO segments are reduced and deposited, and more Li⁺ ions from electrolytes will be reduced on this site to form lithium clusters. When the composite electrode is discharged, the lithium clusters transform into Li⁺ ions to release the extra capacity (see Fig. S4†). Although further research is necessary to verify this process, we believe this finding has made an exciting step toward high capacity lithium storage materials.

Acknowledgements

This work was supported by the National Natural Science Foundation of China (20873029 and 20925312), the State Key Basic Research Program of PRC (2011CB935903), and Shanghai Committee of Science & Technology (09XD1400300, 08DZ2270500 and 09QA1400400).

References

- 1 P. Novak, K. MYller, S. V. Santhanam and O. Hass, *Chem. Rev.*, 1997, **97**, 207.
- 2 K. Nakahara, S. Iwasa, M. Satoh, Y. Morioka, M. Suguro and E. Hasegawa, *Chem. Phys. Lett.*, 2002, **359**, 351.
- 3 J. Qu, T. Katsumata, M. Satoh, J. Wada, J. Igarashi, K. Mizoguchi and T. Masuda, *Chem.–Eur. J.*, 2007, **13**, 7965.
- 4 H. Chen, M. Armand, G. Demailly, F. Dolhem, P. Poizot and J.-M. Tarascon, *ChemSusChem*, 2008, **1**, 348.
- 5 T. Le Gall, H. R. Reiman, M. Grossel and J. R. Owen, *J. Power Sources*, 2003, **119–121**, 316.
- 6 M. Armand, S. Grugeon, H. Vezin, S. Laruelle, P. Ribière, P. Poizot and J.-M. Tarascon, *Nat. Mater.*, 2009, **8**, 120.
- 7 D. E. Fenton, J. M. Parker and P. V. Wright, *Polymer*, 1973, **14**, 589.
- 8 W. H. Meyer, *Adv. Mater.*, 1998, **10**, 439.
- 9 G. S. MacGlashan, Y. G. Andreev and P. G. Bruce, *Nature*, 1999, **398**, 792.
- 10 O. Chusid, Y. Gofer, D. Aurbach, M. Watanabe, T. Momma and T. Osaka, *J. Power Sources*, 2001, **97–98**, 632.
- 11 H. M. Xiong, W. Z. Shen, Z. D. Wang, X. Zhang and Y. Y. Xia, *Chem. Mater.*, 2006, **18**, 3850.
- 12 H. M. Xiong, X. Y. Guan, L. H. Jin, W. W. Shen, H. J. Lu and Y. Y. Xia, *Angew. Chem., Int. Ed.*, 2008, **47**, 4204.
- 13 H. M. Xiong, D. P. Liu, H. Zhang and J. S. Chen, *J. Mater. Chem.*, 2004, **14**, 2775.
- 14 J. Zhu, Z. Lu, S. T. Aruna, D. Aurbach and A. Gedanken, *Chem. Mater.*, 2000, **12**, 2557.
- 15 Y. Kobayashi, M. Okamoto and A. Tomita, *J. Mater. Sci.*, 1996, **31**, 6125.
- 16 S. Maeda and S. P. Armes, *Chem. Mater.*, 1995, **7**, 171.
- 17 J. Jamnik and J. Maier, *Phys. Chem. Chem. Phys.*, 2003, **5**, 5215.
- 18 H. Li, G. Richter and J. Maier, *Adv. Mater.*, 2003, **15**, 736.
- 19 P. Balaya, H. Li, L. Kienle and J. Maier, *Adv. Funct. Mater.*, 2003, **13**, 621.
- 20 H. Li, P. Balaya and J. Maier, *J. Electrochem. Soc.*, 2004, **151**, A1878.
- 21 X. Q. Yu, J. P. Sun, K. Tang, H. Li, X. J. Huang, L. Dupont and J. Maier, *Phys. Chem. Chem. Phys.*, 2009, **11**, 9497.
- 22 J. Hu, H. Li, X. J. Huang and L. Q. Chen, *Solid State Ionics*, 2006, **177**, 2791.